DE GRUYTER OPEN

Eur. Pharm. J. 2017, 64 (2): 9-14.
ISSN 1338-6786 (online) and ISSN 2453-6725 (print version),
DOI: 10.1515/afpuc-2016-0018

EUROPEAN PHARMACEUTICAL JOURNAL

Cation-containing lipid membranes – experiment and md simulations

Original Paper

Kučerka N.,[1,2]✉ Dushanov E.,[3] Kholmurodov KT.,[2,4] Katsaras J.,[5-7] and Uhríková D.[1]

[1]Comenius University in Bratislava, Faculty of Pharmacy, Department of Physical Chemistry of Drugs, Bratislava, Slovak Republic
[2]Frank Laboratory of Neutron Physics, [3]Joint Institute for Nuclear Research, Laboratory of Radiation Biology, Dubna - Moscow Region, Russia
[4]Dubna State University, Dubna Moscow Region, Russia
[5]Oak Ridge National Laboratory, Shull Wollan Center: A Joint Institute for Neutron Sciences, Oak Ridge, Tennessee 37831, United States
[6]Oak Ridge National Laboratory, Biology and Soft Matter Division, Oak Ridge, Tennessee 37831, United States
[7]University of Tennessee, Department of Physics and Astronomy, United States

Received 15 September, 2016, accepted 7 November, 2016

Abstract Using small angle neutron diffraction and molecular dynamics simulations we studied the interactions between calcium (Ca^{2+}) or zinc (Zn^{2+}) cations, and oriented gel phase dipalmitoyl-phosphatidylcholine (DPPC) bilayers. For both cations studied at ~1:7 divalent metal ion to lipid molar ratio (Me^{2+}:DPPC), bilayer thickness increased. Simulation results helped reveal subtle differences in the effects of the two cations on gel phase membranes.

Keywords *Lipid bilayer – metal ions – small angle neutron diffraction – MD simulations – simulation-to-experiment analysis*

INTRODUCTION

Membranes are assemblies of mostly lipids and proteins, biomolecules which are essential to life and act as selective barriers between the cell's interior and exterior environments. In addition, these complex mesoscopic assemblies possess functions which are far more elaborate than a simple permeability barrier populated with proteins. Instead, biomembranes are highly functional dynamic machines that are central to a wide range of biological processes, including the transport of materials, cell defence, recognition, adhesion and signalling. Generally, plasma and organelle membranes serve different functions, as a result, they differ structurally (Kučerka et al., 2015a).

Cell membranes are the first line of defense against invading species, and are key to understanding disease and the efficacy of different pharmaceutical treatments. Small molecules, such as cholesterol (Marquardt et al., 2016), antimicrobial peptides (Pan et al., 2009), fusion peptides (Tristram-Nagle et al., 2010), melatonin (Drolle et al., 2013), vitamin E (Marquardt et al., 2013) and other biomolecules, are able to incorporate into the lipid matrix virtue of the membrane's structure and its associated physical properties (Marquardt et al., 2014). However, the relevant membrane structural properties associated with these processes are often controlled by the presence of certain ions, as all biological processes take place in salt solutions (Petrache et al., 2006) –i.e., the curved bilayers have been shown to undergo a series of structural changes in the presence of Ca^{2+} (Pabst et al., 2007a; Uhríková et al., 2008; Uhríková et al., 2012).

There are a number of experimental approaches used to study biomembranes at the nanoscale. Neutron scattering has proven to be a powerful technique in structural biology and biophysics (Fitter, 2006), including in studies of biological and model lipid membranes. Importantly, recent advances offer unique access to the much touted structure-function

* E-mail: kucerka@fpharm.uniba.sk

relationship in biomembranes, a relationship much sought out in biology and pharmacology (Pabst et al., 2010). Using scattering techniques, changes in the diffraction pattern can indicate important modifications to membrane structure, which may be associated with membrane function (Harroun et al., 2009). For example, small angle neutron diffraction (SAND) revealed increased levels of hydration in bacterial membranes containing Na^+ or Mg^{2+} cations, while Ca^{2+} resulted in less water penetrating the membrane (Kučerka et al., 2008b).

On the other hand, molecular dynamics (MD) simulations, are capable of providing nanoscopic details that are finer than what can be obtained by experiment. More powerful computers and better characterized force fields have made it possible to study larger and more complex systems (Ingolfsson et al., 2014). However, the data from MD simulations are a direct result of the force fields used. It is therefore essential to first validate simulation results with those obtained experimentally (Poger et al., 2016). To this end, the importance of the synergistic relationship between simulation and experiment has become very clear, where simulations are used to aid in the design of models that will ultimately be used to analyse experimental data, and in turn, experimental results are used to improve simulation force fields.

Here, we focus on the well-defined system of dipalmitoyl-phosphatidylcholine (DPPC) membranes containing calcium (Ca^{2+}) or zinc (Zn^{2+}) cations. SAND measurements of oriented multilamellar samples were analysed yielding the one-dimensional structural profile along the membrane normal. Two approaches for the analysis of neutron contrast variation measurements are discussed. In addition, the experimental results are compared to MD simulations. First, a direct simulation-to-experiment comparison was performed in scattering space (Kučerka et al., 2010), while the subsequent examination of the MD data allowed us to identify relevant regions of the membrane in real space.

MATERIALS AND METHODS

1,2-Dipalmitoyl-*sn*-glycero-3-phosphocholine (DPPC) was purchased from Avanti Polar Lipids (Alabaster, AL) and used without further purification. $CaCl_2$ and $ZnCl_2$ salts, and organic solvents were obtained from Fisher Scientific Company (Ontario). The lipid was co-solubilized with appropriate amounts of salt to achieve a stoichiometry of Me^{2+}:DPPC=1:7mol/mol. The dispersions were mixed thoroughly and deposited onto silicon wafers following a well-established procedure (Kučerka et al., 2017). The samples were held at 25 °C during the measurements in an air-tight hydration chamber, based on the original design by Katsaras (Katsaras, 1998). The chamber's bottom was filled with the saturated K_2SO_4 solution prepared at a series of D_2O/H_2O mixtures, resulting in a relative humidity (RH) of 97% (Greenspan, 1977).

Neutron diffraction data were collected at the Canadian Neutron Beam Centre's (CNBC) N5 beamline located at the National Research Universal (NRU) reactor (Chalk River, Ontario, Canada). The diffraction curves were taken using standard symmetric diffraction scans, where scattering space was probed along the *z* direction of the scattering vector *q*. The diffraction curves allow for the reconstruction of one-dimensional neutron scattering length density (NSLD) profiles, as outlined in an earlier study (Kučerka et al., 2009). In addition, rocking curves were collected to evaluate the quality of sample orientation (Nagle et al., 2016).

MD simulations using GROMACS 5.0.4 (Van Der Spoel et al., 2005) were performed at T=298 K on a system of 128 DPPC and 3655 water molecules, while the initial topology was taken from literature (Castillo et al., 2013). Me^{2+} loaded bilayers were constructed by replacing 18 of the water molecules with cations (i.e., Me^{2+}:DPPC=1:7 mol/mol). The GridMAT-MD program (Allen et al., 2009) was used to calculate an average deviation of lipid membrane thickness and an area per lipid, and the radial distribution functions were calculated using the GROMACS auxiliary program. The SIMtoEXP program (Kučerka et al., 2010) was used for the verification of simulated results with those obtained from neutron diffraction experiments.

RESULTS AND DISCUSSION

Compared to the experiment, MD simulations offer increased amounts of information at higher spatial resolution. Specifically, they allow for the identification of individual atoms within the bilayer, and map their locations in 3D space. It should be pointed out, however, that membrane systems are dynamic, and are best described by broad statistical distributions, rather than sharp delta functions typical of perfect crystals (Nagle et al., 2000). 3D simulation data were averaged in the plane of the bilayer, producing 1D distribution functions — no phase separation is expected in the 2D plane of the bilayer. Averaging was also carried out throughout the simulation production time, making the simulation results comparable to those obtained by experiment, which are also averaged over extended periods of time. Finally, we symmetrized all the distributions with respect to the bilayer centre, as any asymmetries should appear as temporary deviations. Typically, the resultant distribution functions from such an analysis are smooth curves. In addition, we combined the distribution functions of individual atoms (united atoms) into components defined by the scattering density profile (SDP) model, which described the studied DPPC bilayers (Kučerka et al., 2008a).

The probability distributions of the different components shown in Fig. 1 reveal typical features of PC bilayers. The bilayer centre is populated almost equally by methyl (CH_3) and methylene (CH_2) groups, and the CH_3 distribution is well-described by a single Gaussian. It is worth noting the absence of strong 'wings', normally seen in disordered bilayers around 15 Å from the bilayer centre (Mihailescu et al., 2011). This implies that the hydrocarbon core of our gel phase DPPC

bilayers is much more ordered. The components describing the PC head group, namely the carbonyl-glycerol (CG) and phosphate-choline (PCN), have maxima at around 17.5 Å, and 22 Å, respectively. The final component shown in Fig. 1 corresponds to the distribution of water whose amplitude achieves half maximum at ~21.6 Å. This value also indicates the lipid-water interface (i.e., the Gibbs dividing surface), or half the bilayer thickness D_B (Kučerka et al., 2008a). Together with a lipid volume of 1143.3 Å^3, as determined from our simulations using the previously derived routine (Petrache et al., 1997), we obtain a lipid area of 53 Å^2.

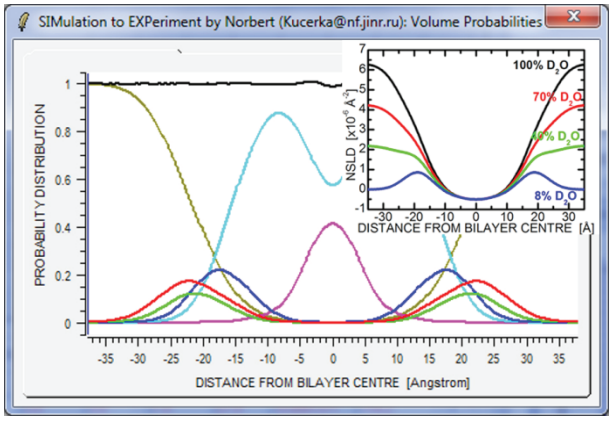

Figure 1. Volume probability distributions determined from MD simulations of neat DPPC bilayers. Atoms are grouped according to the SDP model, which consists, from the bilayer centre outwards, of methyl groups (magenta), methylene (cyan), carbonyl-glycerol (blue), PCN (i.e., phosphate+CH_2CH_2N) (red), and CholCH3 (i.e., choline's CH_3 groups) (green). The inset shows the simulation results in terms of total neutron scattering length density (NSLD) profiles calculated for various contrast conditions (i.e., 100%, 70%, 40%, and 8% D_2O).

MD simulations of systems in which Ca^{2+} or Zn^{2+} cations were added to DPPC bilayers resulted in distributions similar to those shown in Fig. 1. However, Table 1 shows that the bilayer thickness increased by about 1 Å in the case of Ca^{2+}, and decreased in the case of Zn^{2+}. A closer look at the lipid head group components reveals that these changes in bilayer thickness can be attributed to changes in the head group. Specifically, the probability distributions of both the carbonyl and phosphate groups have shifted as a result of cation addition (see Tab. 1). The location can be explained in terms of the preferential interactions between the cations, and the phosphate and carbonyl electronegative oxygens. However, the details of the interactions, which can most likely be related to differences in the electronic structures of the two ions, require further investigation.

The association of the cations with the negatively charged oxygens is further confirmed by the radial distribution functions (RDF) calculated from our simulations. Moreover, they suggest that Ca^{2+} forms contact pairs with phosphate oxygens at about twice the rate of Zn^{2+}. A similar ratio is also

Table 1. Component model structural parameters calculated from MD simulations. Total bilayer thickness D_B is calculated from the Gibbs dividing surface, while the positions of the CG and PCN components are from Gaussian fits.

	D_B [Å]	z_{CG} [Å]	z_{PCN} [Å]
DPPC neat	43.1	17.2	21.1
DPPC:Ca^{2+}	44.4	17.7	21.9
DPPC:Zn^{2+}	42.2	16.7	20.7

observed in the case of the RDF calculated for the carbonyl oxygen. In addition to confirming the preferential interactions of both cations with phosphate, these data indicate a specific binding of Ca^{2+} with the phosphate group, while suggesting a much weaker binding between Zn^{2+} and all other atoms within the lipid head group (Kučerka et al., 2017).

Although our MD results have provided us with some very interesting physical insights, the overall bilayer structural parameters are better determined by experiment. The shortcomings of the different force fields have been previously discussed, particularly with respect to the determination of area per lipid (Kučerka et al., 2010; Valley et al., 2011; Poger et al., 2016). We conducted SAND measurements on the same system as was used for MD simulations to validate the above discussed results. SAND experiments involved contrast variation measurements in which a series of contrast solutions (i.e., 100%, 70%, 40% and 8% D_2O/H_2O) were used. This approach allowed us to solve the scattering phase problem by requiring the scattering form factors to change linearly as a function of D_2O content. The rule arises from the fact that for centro-symmetric systems (as those studied here) scattering intensity is proportional to the square of the contrast between the measured object and the solvent, (Worcester et al., 1976). Once the form factors and their signs are determined, the neutron scattering length density (NSLD) profile is calculated by Fourier transformation (Kučerka et al., 2009). Except for the assumption that the bilayers are centrosymmetric, this procedure inverts the data from reciprocal space into real space without any further assumptions. The 100% D_2O contrast condition provides the best estimate of bilayer steric thickness, while lower contrast profiles reveal more details of the lipid head group region (see inset to Fig. 1). In addition, the contrast varied diffraction data can be subtracted from each other, providing water probability distributions similar to those obtained from MD simulations (Kučerka et al., 2009). Fig. 2 compares these distributions for all three bilayers studied.

Comparison of the simulated and experimental results indicates small differences. Although the simulated data suggest a thickening of the bilayer in the presence of Ca^{2+} ion binding, and a slight decrease in the case of Zn^{2+}, experimental data show a similar effect for both ions. This observation is consistent with previously published results, whereby

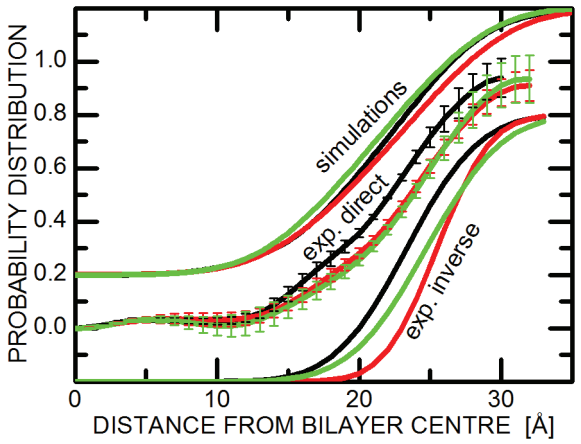

Figure 2. Water probability distributions from simulations (curves shifted up) and by analysis of the experimental data, in real (exp. direct) and reciprocal space (exp. inverse; curves shifted down). The different coloured curves show results for neat DPPC bilayers (black) and those containing Ca^{2+} (red) or Zn^{2+} (green) cations.

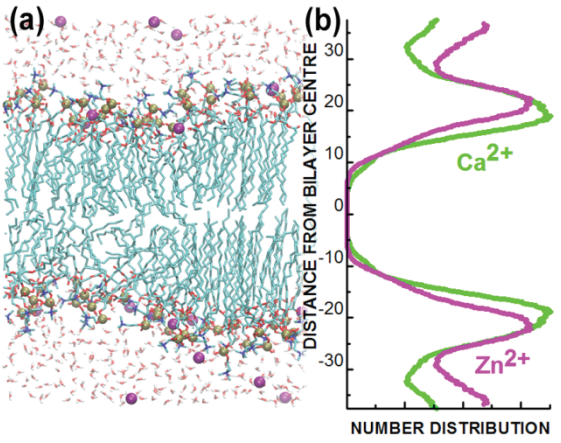

Figure 3. (a) Simulation snapshot of DPPC+Zn^{2+} bilayers showing some of the hydrocarbon chains (low-left part) in the disordered fluid phase, despite a simulation temperature T=298K. (b) The number distribution of Ca^{2+} and Zn^{2+} cations across the DPPC bilayers.

zwitterionic lipid multilayers tend to swell in the presence of salts (Yamada et al., 2005; Petrache et al., 2006; Pabst et al., 2007b; Alsop et al., 2016).

As mentioned, analysis of experimental data in real space does not require any assumptions regarding the NSLD profile functional form, nor of the probability distributions resulting from direct subtraction. The water distribution is obtained from averaging the different contrast varied NSLD profile subtracted pairs, which also provide an estimate of the standard deviation error (Fig. 2). It should be pointed out that these results are, for the most part, qualitative. We used a different approach to analyse the experimental data, producing more quantitative results. This approach evaluates all the different contrast diffraction data simultaneously, while assuming that water probability follows the error function (Kučerka et al., 2009). Results in Fig. 2 show good agreement between the two methods of data analysis. However, our data also highlights the differences between experiment and simulation.

The accuracy of MD simulations is known to vary from study to study, depending on the force field used and the treatment of the electrostatics (Pan et al., 2012). The most difficult aspect for simulations is in reproducing the global membrane parameters due to an imbalance of long range interactions and their approximations, and truncations in the calculations (Kučerka et al., 2015b). As a result, many simulations require an extra variable parameter (e.g., temperature, partial charges, area or surface tension) in order to converge with experiment. For example, we noticed an increased level of disorder in some of the hydrocarbon chains (Fig. 3a), suggesting the spontaneous formation of short-lived fluid phase bilayer regions. This was especially true at the beginning of the simulations. Even though the ordered phase was established during the production run, some fluctuations or other secondary effects may have worked themselves in to our final results.

It is recognized and accepted that atomic-level simulations can provide quantitative details that surpass those obtained from the experiment. These molecular details offer insights into the nature of short-range interactions, hydrogen bridges, and binding specificity. Interatomic correlations also fall into this category, from which we calculated the RDFs between cations and several different atoms within the lipid head group. The data in Fig. 3b shows the presence of strong correlations between Ca^{2+} and the phosphate electronegative oxygen, and also points to the fact that Zn^{2+} cations bind weaker than Ca^{2+} cations (Kučerka et al., 2017). In addition to the RDF results that shed light on the differences between the two cations, the distribution functions agree well with the experimentally obtained results. Despite their subtle differences, Ca^{2+} and Zn^{2+} seem to affect the structural properties of gel phase DPPC bilayers similarly at the concentration examined.

CONCLUSIONS

We used MD simulations and SAND to determine the structural details of DPPC: bilayers containing Ca^{2+} and Zn^{2+} at a lipid:metal molar ratio of 7:1. Simulations were compared to experiments using the simulation-to-experiment approach. Although there is good agreement between simulation and experimental results, SIMtoEXP also shows discrepancies between the two. These differences are not unexpected, and are most likely the result of a less than perfect MD force field. As a result, experimental data were used to determine the overall bilayer structures, which suggest that the addition

of either Ca^{2+} or Zn^{2+} cations induces bilayers to swell. MD simulations, on the other hand, decomposed the bilayer into smaller structural subunits, allowing us to extract important information regarding short-range interactions. It seems that both cations are attracted to the electronegative phosphate and carbonyl moieties of the PC head group. However, Ca^{2+} seems to display an enhanced binding affinity for the phosphate group. Finally, the effects on the bilayer's structural properties at the DPPC:Me^{2+} ratio studied are the same for both cations.

ACKNOWLEDGEMENT

The authors acknowledge support from VEGA grant 1/0916/16, APVV-0212-10, JINR project 04-4-1121-2015/2017, and access to CINS experimental facility and JINR computational heterogeneous cluster HybriLIT. J. K. acknowledges the support received through the Department of Energy (DOE) Scientific User Facilities Division, Office of Basic Energy Sciences (contract no. DEAC05-00OR2275), and funding from the Laboratory Directed Research and Development program.

References

[1] Allen, W. J., Lemkul, J. A., and Bevan, D. R. GridMAT-MD: a Grid-Based Membrane Analysis Tool for Use With Molecular Dynamics. J.Comput.Chem. 2009;30(12):1952-8.

[2] Alsop, R. J., Maria, Schober R., and Rheinstadter, M. C. Swelling of Phospholipid Membranes by Divalent Metal Ions Depends on the Location of the Ions in the Bilayers. Soft Matter 10-8-2016;12(32):6737-48.

[3] Castillo, N., Monticelli, L., Barnoud, J., and Tieleman, D. P. Free Energy of WALP23 Dimer Association in DMPC, DPPC, and DOPC Bilayers. Chem.Phys Lipids 2013;169:95-105.

[4] Drolle, E., Kučerka, N., Hoopes, M. I., Choi, Y., Katsaras, J., Karttunen, M., and Leonenko, Z. Effect of Melatonin and Cholesterol on the Structure of DOPC and DPPC Membranes. Biochimica et Biophysica Acta 2013;1828(9):2247-54.

[5] Fitter, J., Neutron scattering in biology: Techniques and applicationsSpringer-Verlag; 2006.(Gutberlet, T.; Katsaras, J.

[6] Greenspan, Lewis. Humidity Fixed Points of Binary Saturated Aqueous Solutions. JOURNAL OF RESEARCH of the National Bureau of Standards - A.Phys ics and Chemistry 1977;81A(1):89-96.

[7] Harroun, Thad A., Kučerka, Norbert, Nieh, Mu Ping, and Katsaras, John. Neutron and X-Ray Scattering for Biophysics and Biotechnology: Examples of Self-Assembled Lipid Systems. Soft Matter 2009;5(14):2694-703.

[8] Ingolfsson, H. I., Melo, M. N., van Eerden, F. J., Arnarez, C., Lopez, C. A., Wassenaar, T. A., Periole, X., de Vries, A. H., Tieleman, D. P., and Marrink, S. J. Lipid Organization of the Plasma Membrane. J.Am.Chem.Soc. 15-10-2014;136(41):14554-9.

[9] Katsaras, J. Adsorbed to a Rigid Substrate, Dimyristoylphosphatidylcholine Multibilayers Attain Full Hydration in All Mesophases. Biophys.J. 1998;75(5):2157-62.

[10] Kučerka, N., Heberle, F. A., Pan, J., and Katsaras, J. Structural Significance of Lipid Diversity As Studied by Small Angle Neutron and X-Ray Scattering. Membranes (Basel) 2015a;5(3):454-72.

[11] Kučerka, N., Katsaras, J., and Nagle, J. F. Comparing Membrane Simulations to Scattering Experiments: Introducing the SIMtoEXP Software. Journal of Membrane Biology 2010;235(1):43-50.

[12] Kučerka, N., Nagle, J. F., Sachs, J. N., Feller, S. E., Pencer, J., Jackson, A., and Katsaras, J. Lipid Bilayer Structure Determined by the Simultaneous Analysis of Neutron and X-Ray Scattering Data. Biophys.J. 2008a;95(5):2356-67.

[13] Kučerka, N., Nieh, M. P., Pencer, J., Sachs, J. N., and Katsaras, J. What Determines the Thickness of a Biological Membrane. Gen. Physiol Biophys. 2009;28(2):117-25.

[14] Kučerka, N., Papp-Szabo, E., Nieh, M. P., Harroun, T. A., Schooling, S. R., Pencer, J., Nicholson, E. A., Beveridge, T. J., and Katsaras, J. Effect of Cations on the Structure of Bilayers Formed by Lipopolysaccharides Isolated From Pseudomonas Aeruginosa PAO1. J.Phys Chem.B 10-7-2008b;112(27):8057-62.

[15] Kučerka, N., van Oosten, B., Pan, J., Heberle, F. A., Harroun, T. A., and Katsaras, J. Molecular Structures of Fluid Phosphatidylethanolamine Bilayers Obtained From Simulation-to-Experiment Comparisons and Experimental Scattering Density Profiles. The Journal of Physical Chemistry B 5-2-2015b;119(5):1947-56.

[16] Kučerka, N., Dushanov, E., Kholmurodov, K. T., Katsaras, J., and Uhríková, D. Calcium and Zinc Differentially Affect the Structure of Lipid Membranes. Langmuir 2017;33:3134-3141.

[17] Marquardt, D., Kučerka, N., Wassall, S. R., Harroun, T. A., and Katsaras, J. Cholesterol's Location in Lipid Bilayers. Chem.Phys Lipids 2016;199:17-25.

[18] Marquardt, D., Williams, J. A., Kučerka, N., Atkinson, J., Wassall, S. R., Katsaras, J., and Harroun, T. A. Tocopherol Activity Correlates With Its Location in a Membrane: a New Perspective on the Antioxidant Vitamin E. J.Am.Chem.Soc. 22-5-2013;135(20):7523-33.

[19] Marquardt, Drew; Harroun, Thad A. Locations of Small Biomolecules in Model Membranes. Liposomes, Lipid Bilayers and Model Membranes.CRC Press; 19-2-2014. pp.199-216.

[20] Mihailescu, M., Vaswani, R. G., Jardon-Valadez, E., Castro-Roman, F., Freites, J. A., Worcester, D. L., Chamberlin, A. R., Tobias, D. J., and White, S. H. Acyl-Chain Methyl Distributions of Liquid-Ordered and -Disordered Membranes. Biophys.J. 16-3-2011;100(6):1455-62.

[21] Nagle, J. F., Akabori, K., Treece, B. W., and Tristram-Nagle, S. Determination of Mosaicity in Oriented Stacks of Lipid Bilayers. Soft Matter 14-2-2016;12(6):1884-91.

[22] Nagle, J. F. and Tristram-Nagle, S. Structure of Lipid Bilayers. Biochimica et Biophysica Acta 10-11-2000;1469(3):159-95.

[23] Pabst, G., Hodzic, A., Strancar, J., Danner, S., Rappolt, M., and Laggner, P. Rigidification of Neutral Lipid Bilayers in the Presence of Salts. Biophys.J. 15-10-2007a;93(8):2688-96.

[24] Pabst, G., Hodzic, A., Strancar, J., Danner, S., Rappolt, M., and Laggner, P. Rigidification of Neutral Lipid Bilayers in the Presence of Salts. Biophys.J. 15-10-2007b;93(8):2688-96.

[25] Pabst, G., Kučerka, N., Nieh, M. P., Rheinstadter, M. C., and Katsaras, J. Applications of Neutron and X-Ray Scattering to the Study of Biologically Relevant Model Membranes. Chem.Phys Lipids 2010;163(6):460-79.

[26] Pan, J., Heberle, F. A., Tristram-Nagle, S., Szymanski, M., Koepfinger, M., Katsaras, John, and Kučerka, N. Molecular Structures of Fluid Phase Phosphatidylglycerol Bilayers As Determined by Small Angle Neutron and X-Ray Scattering. Biochimica et Biophysica Acta 2012;1818(9):2135-48.

[27] Pan, J., Tristram-Nagle, S., and Nagle, J. F. Alamethicin Aggregation in Lipid Membranes. Journal of Membrane Biology 2009;231(1):11-27.

[28] Petrache, H. I., Feller, S. E., and Nagle, J. F. Determination of Component Volumes of Lipid Bilayers From Simulations. Biophys.J. 1997;72(5):2237-42.

[29] Petrache, H. I., Tristram-Nagle, S., Harries, D., Kučerka, N., Nagle, J. F., and Parsegian, V. A. Swelling of Phospholipids by Monovalent Salt. J.Lipid Res. 2006;47(2):302-9.

[30] Poger, D., Caron, B., and Mark, A. E. Validating Lipid Force Fields Against Experimental Data: Progress, Challenges and Perspectives. Biochimica et Biophysica Acta 2016;1858(7 Pt B):1556-65.

[31] Tristram-Nagle, S., Chan, R., Kooijman, E., Uppamoochikkal, P., Qiang, W., Weliky, D. P., and Nagle, J. F. HIV Fusion Peptide Penetrates, Disorders, and Softens T-Cell Membrane Mimics. J.Mol.Biol. 10-9-2010;402(1):139-53.

[32] Uhríková, D., Kučerka, N., Lengyel, A., Pullmannová, P., Teixeira, J., Murugova, T., Funari, S. S., and Balgavý, P. Lipid Bilayer - DNA Interaction Mediated by Divalent Metal Cations: SANS and SAXD Study. Journal of Physics: Conference Series 2012;351(1):012011.

[33] Uhríková, D., Kučerka, N., Teixeira, J., Gordeliy, V., and Balgavý, P. Structural Changes in Dipalmitoylphosphatidylcholine Bilayer Promoted by Ca2+ Ions: a Small-Angle Neutron Scattering Study. Chem.Phys Lipids 2008;155(2):80-9.

[34] Valley, C. C., Perlmutter, J. D., Braun, A. R., and Sachs, J. N. NaCl Interactions With Phosphatidylcholine Bilayers Do Not Alter Membrane Structure but Induce Long-Range Ordering of Ions and Water. Journal of Membrane Biology 2011;244(1):35-42.

[35] Van Der Spoel, D., Lindahl, E., Hess, B., Groenhof, G., Mark, A. E., and Berendsen, H. J. GROMACS: Fast, Flexible, and Free. J.Comput.Chem. 2005;26(16):1701-18.

[36] Worcester, D. L. and Franks, N. P. Structural Analysis of Hydrated Egg Lecithin and Cholesterol Bilayers. II. Neutrol Diffraction. J.Mol.Biol. 25-1-1976;100(3):359-78.

[37] Yamada, L., Seto, Hideki, Takeda, Takayoshi, Nagao, Michihiro, Kawabata, Youhei, and Inoue, Katsuaki. SAXS, SANS and NSE Studies on "Unbound State" in DPPC/Water/CaCl2 System. Journal of the Physical Society of Japan 15-10-2005;74(10):2853-9.